

Use of two deformable mirrors AO system for an Interferometric test-bed

Sergio R. Restaino¹, Dave V. Wick², Ty Martinez³, Don T. Payne⁴, G. Charmaine Gilbreath¹

¹ Naval Research Laboratory
Remote Sensing Division, Code 7215
3550 Aberdeen SE, Albuquerque, NM 87117 USA
Sergio.Restaino@kirtland.af.mil

² Sandia National Laboratory
PO Box 5800, MS 1188
Albuquerque NM, 87185 USA

³ Air Force Research Laboratory,
Directed Energy Directorate
3550 Aberdeen SE
Albuquerque NM, 87117 USA

⁴ Narrascope
3101 Hyder SE
Albuquerque NM 8106 USA

ABSTRACT

In this paper, we present results on a test-bed for the use of adaptive optics (AO) in optical interferometry. The test-bed is based on two deformable mirrors made by OKO technologies. The two mirrors are simultaneously controlled by the same computer and control software. The experimental set is based on our portable adaptive optics system. The goal of this test-bed is to study and characterize the effects of aberrations on the fringe contrast and the effects and characterization of the use of AO for improving fringe contrast. In this paper we will report some field test of our portable AO system. We will also describe the test-bed and some of the experimental results obtained so far.

1. INTRODUCTION

One of the main aims of our group is the study of improvements to optical interferometry using adaptive optics. In order to analyze various capabilities and study the trade-off parameter space we have set-up three parallel efforts: an analytical effort, see [1], a field effort and a laboratory effort. Results are presented from a compact, portable Adaptive Optics (AO) system. The initial results presented in this paper show data from a system whose design approach views the AO system as a self-contained

instrument much like a camera or a spectrograph rather than as a part of the infrastructure of the telescope, which is the traditional view. The goal of this ongoing work is to create a versatile, accessible approach for various current users and various new users of adaptive optics technologies and those investigators interested in improving the response of their telescopes by correcting the effects of the atmosphere. Of specific interest, is the development of a compact, lightweight, low cost AO system that can be deployed on multiple telescopes configured as an interferometer. This system is characterized by flexibility and robustness that allows portability, simple mounting; ease of alignment and calibration procedures; and adaptability to readily exchange different types of Deformable Mirrors (DM) and wavefront sensors. Customized software and hardware combined with commercially available optics, camera, DM, and wavefront sensor provided a low cost, compact alternative to conventional systems. Some of the key features of the reconstructor allow to transportability by reducing or eliminating the need for tight alignment between the wavefront sensor, the camera and the corrective element. Furthermore, unlike more conventional approaches, this system is designed to recover quickly from loss of data, i.e. missing frames, to continue operations even under non-favorable conditions. Such characteristic is also central to the ability of the system to cope with the effects of scintillation. In the following sections we will examine some field data and report on the results. Furthermore, in this paper we present results of our two mirror test-bed. Such test-bed is uniquely suited for the study of interaction between AO and optical interferometry (OI).

2. The Portable AO System

Several authors are interested lately in low cost adaptive optical systems, see for example [2,3], and the characteristics and performances of such systems are becoming more readily available. In this section we will briefly describe our system and some of the field results obtained in a couple of observing runs at different, meter class telescopes.

The AO system was tested during an engineering run in July 2002 using the one-meter telescope at the Naval Observatory Flagstaff Station (NOFS) as shown in Figure 1.

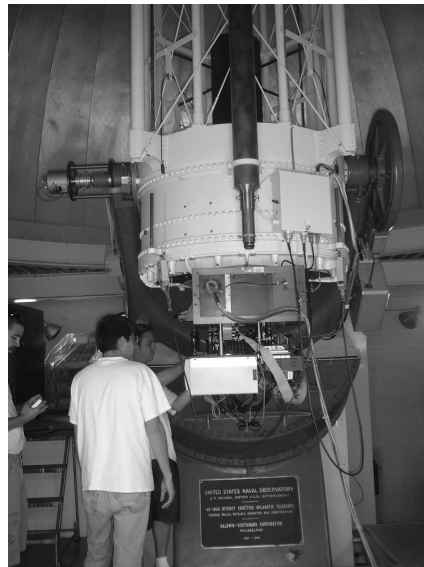


Figure 1. Compact Adaptive Optics system being installed on one-meter telescope at the Naval Observatory Flagstaff Station.

The observing run was during the monsoon season. Although the seeing was poor, it was sufficient to test the optical layout and the closed loop performance of the software. Data were taken on α Lyrae (Vega) between clouds and through haze during two nights. In the middle of the first night, the AO system was removed and a CCD camera was placed in the focal plane of the telescope optics train in order to calibrate the system using a standard NOFS camera. The AO system was then reinstalled.

The system was mounted on an 18x24 inch, .75 inch thick aluminum plate. The optics resides on top of the plate while the power supply and computer are mounted to the bottom of the plate. The adaptive element used in this experiment was a MEM 37-element mirror [4] from OKO technologies. The unit is 15 mm diameter and was driven with custom electronics to drive each actuator with 0V-140V providing a "throw" of approximately 60 waves (at 633 nm) for focus and about 2-1/2 waves for higher order corrections. Real-time data acquisition and control interfaces for the unit was provided by BAO and reconstructor and control algorithms were developed by Narrascape for PC-based control. The DM and schematic of the MEM mirror are shown in Figure 2.

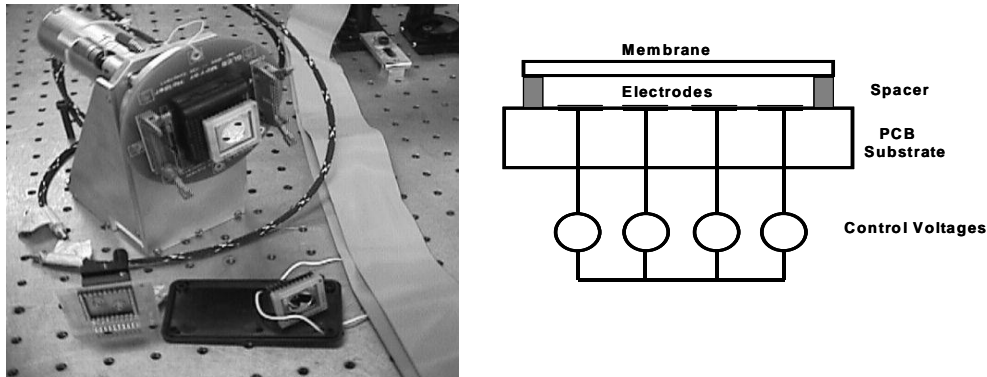


Figure 2. Photo and schematic of OKO deformable mirror used in described adaptive optics system. This unit has 37 active elements and measures 15 mm in diameter. Custom electronics drove the actuators.

The wavefront sensor was a Shack-Hartman lenslet array coupled to a 128 pixel square Dalsa CCD camera. The maximum allowed frame-rate for such camera and read-out electronics is of approximately 800 frames per second. The camera read-out noise, especially at high frame-rates, was the limiting factor for the sensitivity of the system. Combined with the poor seeing conditions, due in large part to high clouds on the one available night during the run, the performance of the Dalsa in this mode required actual frame rates to be around 100 Hz. For a brief period during the observing run, the weather cleared enough to close the loop on the bright star Vega.

The telescope itself presented a challenge to the wavefront reconstruction algorithm. The pupil of the telescope has a 45% central obscuration due to the secondary mirror. This is

Sixty subapertures were used for wavefront sensing. The wavefront reconstructor required at least three subapertures between the inner and outer radii. Figure 3 shows both the pupil and the images formed by the subapertures. The 45% obscuration by the secondary is evident in both images.

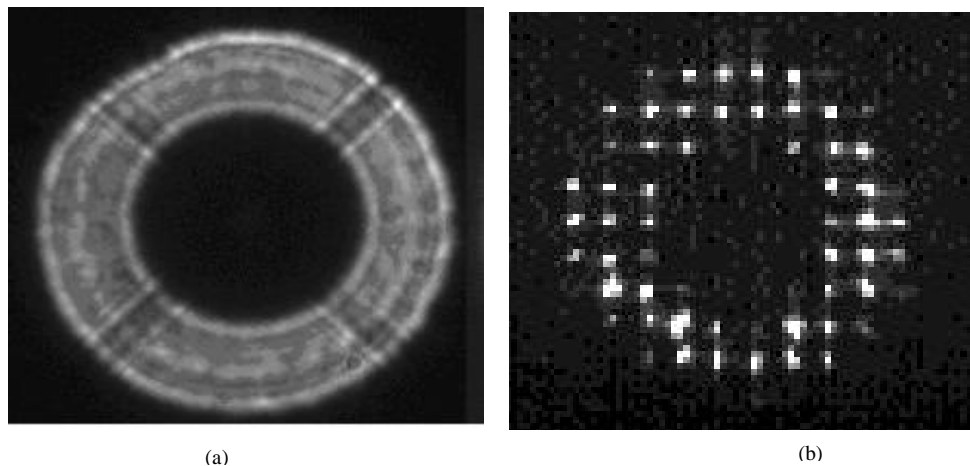


Figure 3. (a) Pupil imaged; large secondary evident; (b) Single frame from the wavefront sensor camera.

The Shack-Hartman measurements and data processing, are illustrated in Eqn.s 1 and 2.

$$\Delta x = \frac{R}{n} \frac{\partial \phi}{\partial x} \quad \Delta y = \frac{R}{n} \frac{\partial \phi}{\partial y} \quad 1$$

$$s = [B]\phi + n \quad 2$$

$$\phi = [B^1 C_n B]^{-1} [B^T] [C_n]^{-1} s \quad 3$$

Equation 1 represents the slope measurements made by a Shack-Hartmann sensor. Eq. 2 is the signal equation of the wavefront sensor, where the matrix B is the reconstructor matrix and n represents the noise. The least square approach to invert eq. 2 is shown in eq. 3 under generic assumptions, i.e. that we can use a covariance matrix to describe the noise contribution C_n , etc. This traditional reconstruction scheme, however, has difficulties with missing data, especially when they are dynamically changing like in the case of scintillation. However, with our new algorithm, the reconstructor is not vulnerable to effects from large obscurations, and the effects of scintillation. This was one of the reasons that we elected to observe in the middle of the monsoon season in Flagstaff, to evaluate the effects of scintillation on our new reconstructor algorithm. The new algorithm will be the object of a forthcoming publication.

Measurements of scintillation index were carried out using the wavefront sensor data. The scintillation index, for definition and properties see for example ref. [4], is typically around 20% and for very good *seeing* conditions it is of only few percent. Fig. 4 shows a 3.5 seconds time sequence of four subapertures. The measured scintillation index, averaged over the sub-pupils, is shown in figure 5.

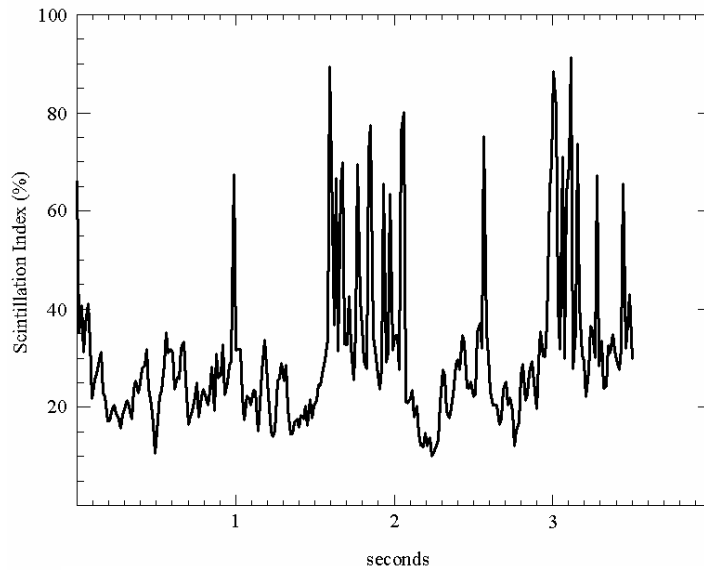


Figure 4: scintillation index vs. time

A few seconds video of the raw data from the wavefront sensor CCD camera is shown in figure 6.

The analysis of figures 4, 5 and 6 illustrates the amount of scintillation that the reconstructor had to cope with. Notwithstanding such dynamical changes in the number of illuminated subapertures, as can be clearly seen in the video in fig. 6, the reconstructor was able to allow closed loop operations. Scintillation and poor seeing decreases the stability of the wavefront reconstruction since the variation in intensity makes for large differences in the signal-to-noise ratio from one sub-pupil to another. Cloud cover made observations logistically challenging. Images of Vega using open and closed loop corrective optics are shown in Figures 7a and 7b.

The images are 30 second integrations. The closed-loop point spread function (PSF) is symmetric and the central peak is much higher. A scan through the vertical axis of fig. 7 is shown in fig. 8 and the scale is in counts, after bias and dark correction, of the CCD camera. The time averaged open-loop Strehl ratio was about 3.7% and the closed-loop Strehl ratio was 27%, showing a factor of 6 in improvement, even with the difficult conditions. Figure 9 shows a single frame non-time averaged, open loop and closed-loop, of Vega. The instantaneous Strehl ratios are 2.9% and 21% respectively.

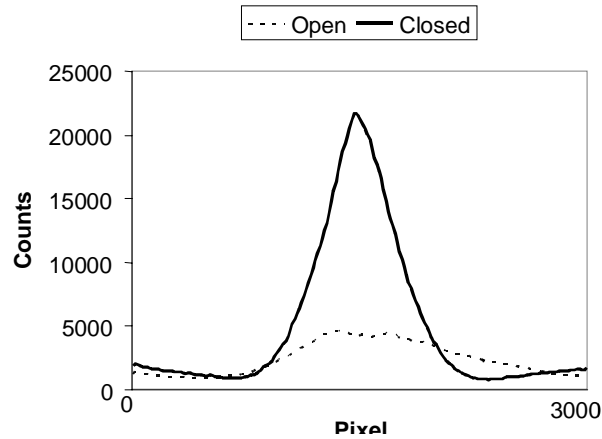


Figure 5: Cross-cur of the two PSF shown in fig. 7

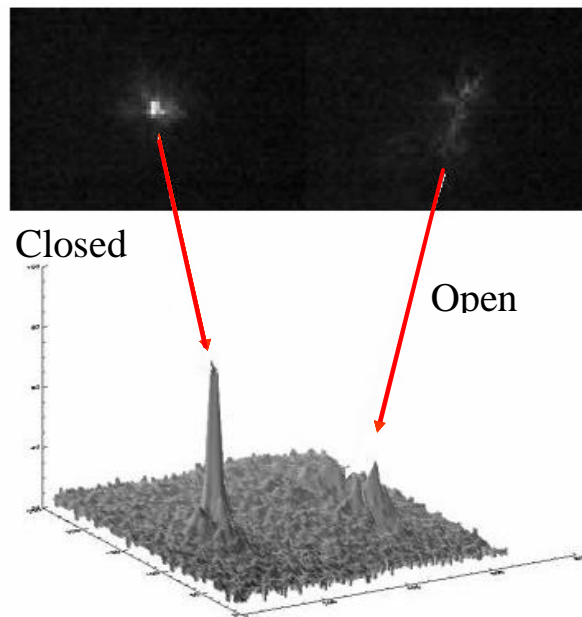


Figure 6: Single frame open closed and open loop

3. The Two Deformable Mirrors Test-Bed.

From our portable AO system we have developed a two deformable mirrors test-bed to study various problems inherent to the interaction and performances of AO with OI. A schematic lay-out of the test-bed is illustrated in figure 7.

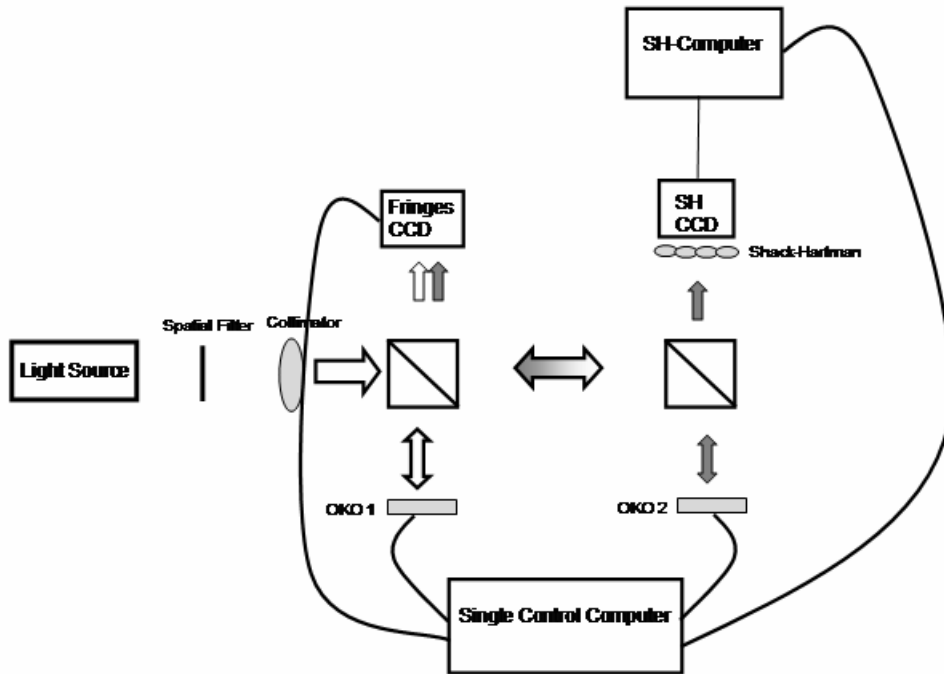


Figure 7: schematic lay-out of the two mirrors test-bed.

The deformable mirrors used are two OKO 59 actuators with a clear aperture of 30 mm. A series of experiments were carried out where a very accurate measurement of the wavefront aberrations were performed using a Shack-Hartman wavefront sensor monitoring the *aberrating* OKO mirror. In figure 8 and 9 are shown some examples of the amplitude, in waves, of a Zernike polynomial decomposition of the wavefronts before and after correction. The first wavefront is measured by the Shack-Hartmann and a standard Zernike polynomial expansion, up to 24 terms, is carried out. The second wavefront is inferred from the interference fringes after correction is applied to the second mirror. The solid line is the aberrated wavefront decomposition, and the dashed line is the corrected one. The piston term is not included in the expansion.

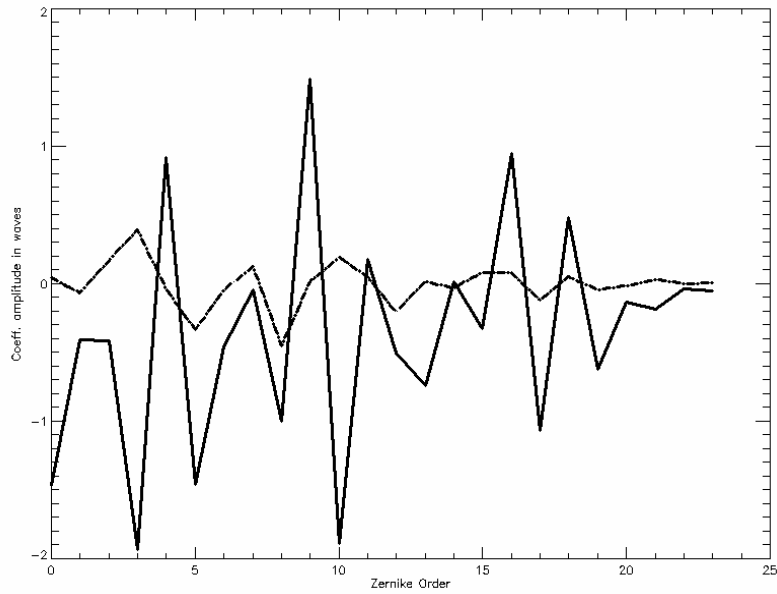


Figure 8: amplitude of the Zernike coefficients polynomial expansion

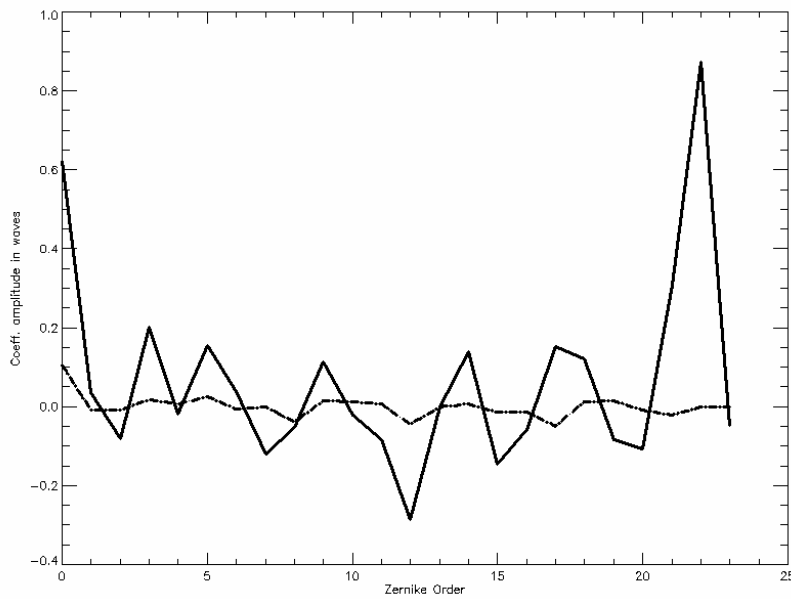


Figure 9: Same as in Fig. 8, different realization.

At this point we can look at the fringe contrast in function of rms wavefront error. The correction of the wavefront done by the second mirror is not perfect due to various reasons. First of all the measurement of the wavefront

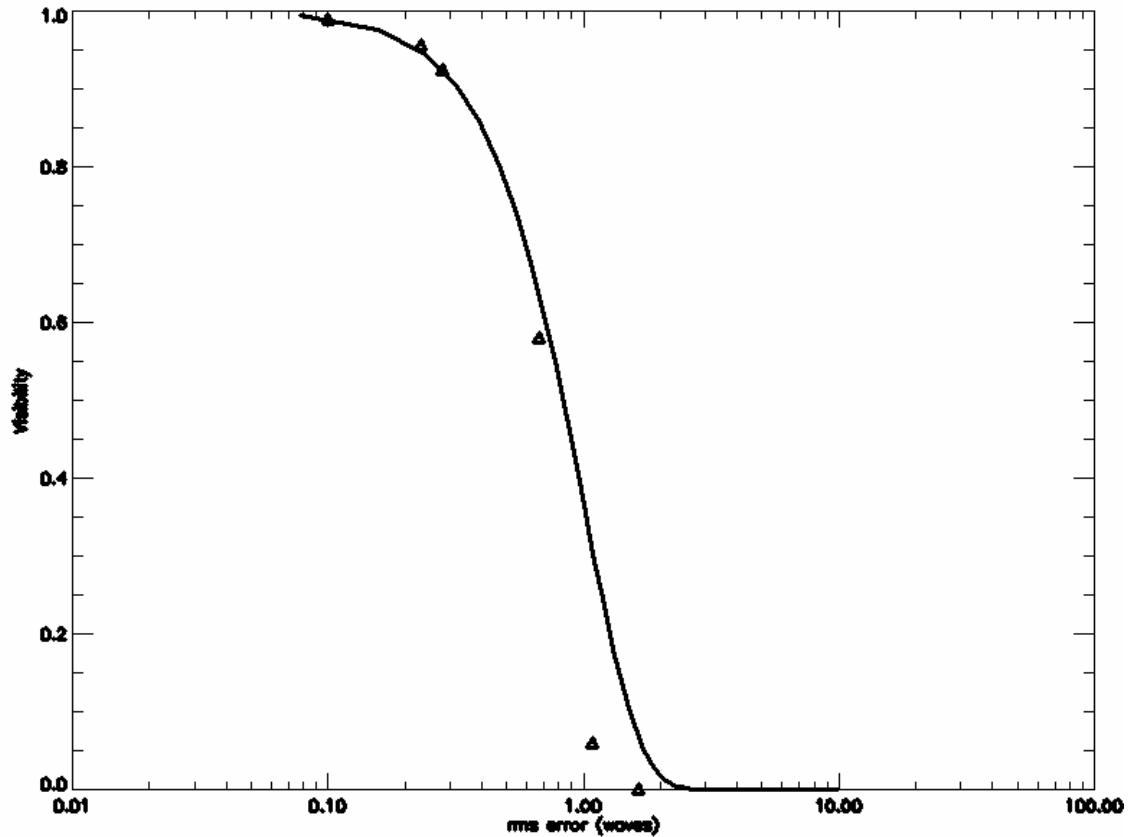


Figure 10: Measured fringe visibility vs. rms wavefront error (triangles), exponential fit (solid line)

The points are the average fringe visibility of several measurements in function of the rms error, in waves, of the wavefront. The solid line indicates an exponential fit of the type $\exp(-\sigma^2)$. The fit, as expected is very good for very small rms errors. The most important aspect, however, of our test-bed is twofold. On one side it will allow us to test novel control algorithms that currently under development in our group [6], on the other the study of the effect of partial adaptive optics correction on fringe visibility. The region of interest it is around a wavefront variance of approximately 0.5λ .

4. Summary

In this paper we have presented some preliminary results from our adaptive optics program for optical interferometry. The program hinges on four components: a theoretical and analytical study, subject of a paper in these proceedings; an analytical/experimental study on novel control algorithms, also subject of a paper in these proceedings; an experimental test-bed to study these interactions in the laboratory environment; and last, but not least, our field experiments. Here we have discussed some field results of our AO system and some preliminary results of the lab test-bed.

5. REFERENCES

1. Mozurkewich D., Restaino S.R., Gilbreath GC, "Adaptive Optics and Optical Interferometry" these proceedings.
2. Paterson C., Munro I., Dainty J.C.; "A low cost adaptive optics system using a membrane mirror", Opt. Exp. **6**(9), 175-185 (2000)
3. S.R. Restaino, G.C. Gilbreath, D.T. Payne, J. Andrews, "Experimental Results of a MEM Based Adaptive Control Systems," Proc. SPIE Vol. **5348**, 160
4. Zhu L. *et al.*, "Active control of a micromachined continuous-membrane deformable mirror for aberration compensation", App. Opt. **38** 168-176 (1999)
5. Roddier F., "The effects of atmospheric turbulence in optical astronomy", Progress in Optics XIX, 281-376 (1981)
6. Cristi, R., Restaino S.R., LeBlanc J.L., "Optimal distributed prediction and estimation controller with application to adaptive optics and optical interferometry", these proceedings.